

# Curved waveguide grating demultiplexer (CWG) with a flattened response via bimodal output waveguides

(Student paper)

Abdelfettah Hadij-ElHouati,<sup>1,\*</sup> Robert Halir,<sup>1</sup> Alejandro Ortega-Moñux,<sup>1</sup> J. Gonzalo Wangüemert-Pérez,<sup>1</sup>

Jens H. Schmid,<sup>2</sup> Pavel Cheben,<sup>2</sup> and Iñigo Molina-Fernandez<sup>1</sup>

<sup>1</sup>Telecommunication Research Institute (TELMA), Universidad de Málaga, CEI Andalucía TECH, Louis Pasteur 35, 29010 Málaga, Spain

<sup>2</sup>National Research Council Canada, Ottawa, Ontario K1A 0R6, Canada

\* abdel@uma.es

**We demonstrate a compact wavelength demultiplexer for the silicon-on-insulator platform based on the curved waveguide grating (CWG) architecture. The proposed device uses bimodal output waveguides to achieve a low-loss flattened spectral response. The device shows insertion loss as low as 1.2 dB and crosstalk below -20 dB.**

**Keywords:** WDM demultiplexer, curved waveguide grating, SOI, SWG, flat-top

## INTRODUCTION

Silicon photonics (SiPh) has become the leading integrated photonics technology [1]. It brings together high integration density while being compatible with the already established microelectronic CMOS process allowing low-cost mass production. Datacom is an important application area of SiPh [2]. Wavelength division multiplexing (WDM) data links are used to achieve high aggregated data rates without increasing the symbol rates, which are limited by the modulator and demodulator bandwidths. The wavelength (de)multiplexer is a key component in WDM systems. Various WDM demultiplexing schemes have been proposed for the SiPh platform including ring resonator filters, lattice-form filters, arrayed waveguide gratings (AWGs) and echelle gratings (EGs) [3]. Flattened spectral response is highly desired for demultiplexers as it reduces the spectral stability requirements of the laser, hence reducing the laser cost and avoiding the need for thermal control.

The curved waveguide grating (CWG) demultiplexer was proposed by Hao et al. as a promising alternative to the conventional architectures [4] and was later demonstrated for the silicon-on-insulator (SOI) platform at the National Research Council Canada [5], [6]. We recently demonstrated a low-loss CWG demultiplexer that achieves state-of-the-art performance [7]. In that work, we use the single-beam condition [8] to suppress the off-chip radiation that causes optical loss [9]. For doing so, we judiciously design the diffractive grating period and the lateral subwavelength grating (SWG) slab metamaterial to frustrate phase-matching in the silica while allowing it in the SWG slab. Figure 1 shows a schematic of the proposed CWG demultiplexer comprising: a curved waveguide grating placed along a circular path, SWG a slab, a free propagation region (FPR) slab and output receiving waveguides positioned on the so-called Rowland circle. The SWG slab is a periodic structure that synthesizes an artificial metamaterial with a properly designed effective refractive index [10], [11].

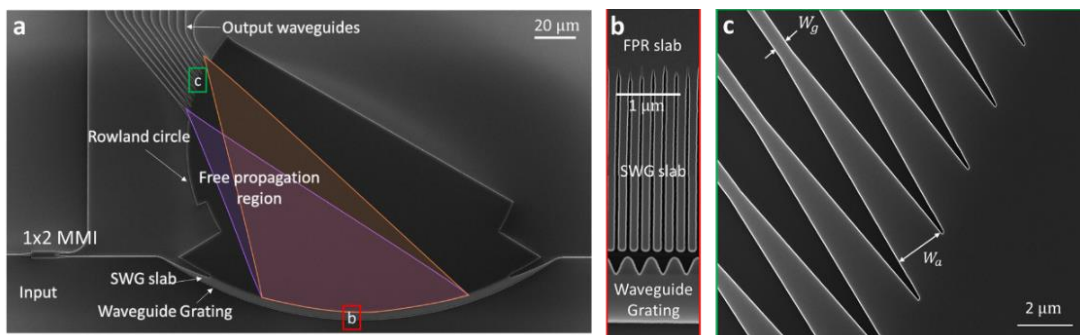


Fig. 1. Curved waveguide grating demultiplexer schematic (a), detail of the sinusoidal waveguide grating (b) and detail of the receiving waveguides and tapers (c).

Here, we present a low loss CWG demultiplexer with a flattened response that uses the first two modes of the output waveguides to achieve a low loss flattop response [3]. The device efficiently separates 5 channels spaced 10nm within C-band with an insertion loss as low as 1.2 dB and crosstalk better than -20 dB.

## FUNDAMENTALS AND DESIGN

The TE polarized light entering the device from the input waveguide is progressively diffracted by the waveguide grating. The SWG region guides the diffracted light into the FPR. The light propagates through the FPR and is focused on the Rowland circle where is captured by the receiving apertures of width  $W_a$  that are tapered to the output waveguides of width  $W_g$  (see Fig. 1c). The dispersive nature of the waveguide grating produces the demultiplexing functionality since the diffraction angle  $\theta$  varies with the wavelength as described by the grating equation:

$$\theta(\lambda) = \text{asin}((n_{FB} - \lambda/\Lambda)/n_S) \quad (1)$$

where,  $n_{FB}$  is the waveguide grating Floquet-Bloch mode effective index,  $\lambda$  is the free-space wavelength,  $\Lambda$  is the waveguide grating period and  $n_S$  is the effective index of the FPR slab. To fulfil the single beam condition [8], output waveguides are placed at an angle  $\theta \approx -35^\circ$  from the grating normal.

The CWG demultiplexer was designed following the same procedure as the Gaussian-shaped device reported in [7]. The grating radius was set to  $R = 230 \mu\text{m}$  to enforce a channel separation of 10 nm. To limit the grating length to  $\pi/3$  rad along the grating circle, the illumination spot at the focal plane was set to a Gaussian with a mode field radius (MFR) of  $0.75 \mu\text{m}$ , which corresponds to the fundamental mode of a  $2.15\text{-}\mu\text{m}$  width waveguide. For this illumination, we have evaluated the transmission response as a function of the spectral shift normalized to the 25-dB bandwidth (shown in Fig. 2) for both the monomodal (grey curve) and bimodal output waveguides cases (coloured curves). We observe that the response is flattened for the bimodal case as the taper width  $W_a$  is increased. We also include, for reference, the response when a mono-mode output is used with a taper width matched to the illumination ( $W_a = 2.15 \mu\text{m}$ ).

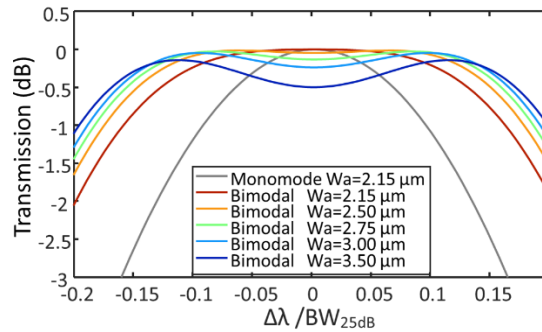


Fig. 2. Channel response for mono-mode (grey) and bimodal outputs (colour) for various widths of the receiving tapers  $W_a$ .

Figure 3 shows the response characteristics as a function of the taper width  $W_a$ . To measure flatness, we used the ratio of 25-dB and 1-dB bandwidths, shown in Fig. 3.a. We see that by increasing the taper width  $W_a$ , the flatness improves when using bimodal outputs (purple) and stays unaltered for the mono-mode outputs (grey). However, this also raises the ripple (Fig. 3.b) and loss (Fig. 3c). We use  $W_a = 2.75 \mu\text{m}$  as a compromise value to attain twice the flatness while incurring a negligible impact on the loss ( $<0.2$  dB) and ripple ( $<0.2$  dB). The output waveguides width  $W_g$  was set to 700 nm, ensuring low-loss propagation for the two first TE modes while frustrating higher-order modes propagation.

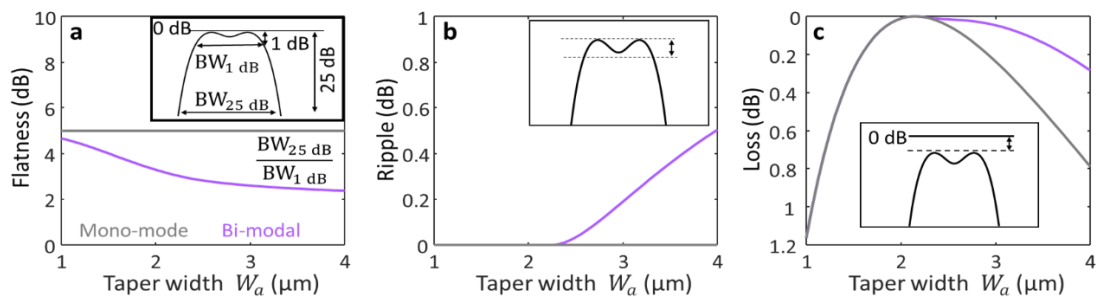


Fig. 3. Response characteristics for a bimodal output CWG (purple) compared with a mono-mode output (grey). a) Flatness, b) ripple and c) loss when the CWG focuses a  $0.75\text{-}\mu\text{m}$ -MFR Gaussian illumination at the receiving tapers versus their width  $W_a$ .

## EXPERIMENTAL VERIFICATION

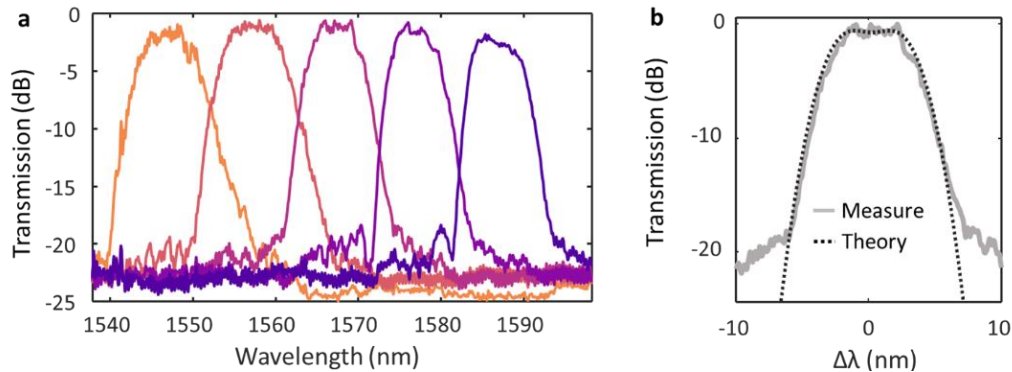


Fig. 3. a) Measured spectra for the fabricated CWG demultiplexer with flat-top response. b) Comparison of a selected channel response with the designed theoretical response shape.

The device was fabricated in a standard SOI platform wafer using electron beam lithography patterning and reactive ion etching.

The characterization was done by injecting a monochromatic, TE-polarized signal from a tuneable laser and measuring the signal power at the output waveguides with a photodetector. An on-chip 3dB power splitter was used at the device input to extract a reference signal to determine the device transmittance (see Fig. 1a). Figure 4 shows the measured transmission spectra for the device. The response shape matches the theoretical flat-top response as shown in Fig. 4.b. The measured losses range from 1.2 dB to 2 dB and the crosstalk is lower than -20 dB for all channels.

## CONCLUSIONS

We have demonstrated a low-loss flat-top 5-channel curved waveguide grating wavelength demultiplexer for the SOI platform. The off-chip radiation was virtually suppressed by enforcing the single beam condition on the grating waveguide using metamaterial refractive index engineering while flat-top response was achieved via bi-modal output waveguides. The experimental device exhibits flattened spectral response while maintaining low loss (1.2-2 dB) and crosstalk (<-20 dB).

Acknowledgements: Universidad de Málaga; Ministerio de Educación, Cultura y Deporte (MECD) (FPU16/03401), Ministerio de Ciencia, Innovación y Universidades (MCIU) (PID2019-106747RBI00), Consejería de Economía, Conocimiento, Empresas y Universidad (CECEU) (UMA18-FEDERJA-219, P18-RT1453, P18-RT-793).

## References

- [1] D. Thomson *et al.*, 'Roadmap on silicon photonics', *J. Opt.*, vol. 18, no. 7, p. 073003, Jul. 2016.
- [2] Z. Zhou, R. Chen, X. Li, and T. Li, 'Development trends in silicon photonics for data centers', *Optical Fiber Technology*, vol. 44, pp. 13–23, Aug. 2018.
- [3] K. Okamoto, 'Wavelength-Division-Multiplexing Devices in Thin SOI: Advances and Prospects', *IEEE J. Select. Topics Quantum Electron.*, vol. 20, no. 4, pp. 248–257, Jul. 2014.
- [4] Y. Hao *et al.*, 'Novel dispersive and focusing device configuration based on curved waveguide grating (CWG)', *Opt. Express*, vol. 14, no. 19, p. 8630, 2006.
- [5] J. H. Schmid *et al.*, 'Refractive Index Engineering With Subwavelength Gratings in Silicon Microphotonic Waveguides', *IEEE Photonics J.*, vol. 3, no. 3, pp. 597–607, Jun. 2011.
- [6] P. J. Bock *et al.*, 'Demonstration of a curved sidewall grating demultiplexer on silicon', *Opt. Express*, vol. 20, no. 18, p. 19882, Aug. 2012.
- [7] A. Hadij-Elhouati *et al.*, 'Low-loss off-axis curved waveguide grating demultiplexer', *Opt. Lett.*, vol. 46, no. 19, p. 4821, Oct. 2021.
- [8] A. Hadij-Elhouati *et al.*, 'High-efficiency conversion from waveguide mode to on-chip beam using a metamaterial engineered Bragg deflector', *Opt. Lett.*, vol. 46, no. 10, pp. 2409–2412, May 2021.
- [9] A. Hadij-Elhouati *et al.*, 'Distributed Bragg deflector coupler for on-chip shaping of optical beams', *Opt. Express*, vol. 27, no. 23, pp. 33180–33193, Nov. 2019.
- [10] P. Cheben *et al.*, 'Subwavelength integrated photonics', *Nature*, vol. 560, no. 7720, pp. 565–572, Aug. 2018.
- [11] J. M. Luque-González *et al.*, 'A review of silicon subwavelength gratings: building break-through devices with anisotropic metamaterials', *Nanophotonics*, vol. 10, no. 11, pp. 2765–2797, Aug. 2021.